ISIJ International, Vol. 51 (2011), No. 11, pp. 1831–1837

Suppression of Coarse Columnar Grain Formation in As-cast Austenite Structure of a Hyperperitectic Carbon Steel by Nb Addition

Munekazu OHNO,[1)] Tetsuya YAMAGUCHI,[2)] Kiyotaka MATSUURA[1)] and Kohichi ISOBE[3)]

1) Division of Materials Science and Engineering, Faculty of Engineering, Hokkaido University, Kita 13 Nishi 8, Kita-ku, Sapporo, Hokkaido 060-8628 Japan. 2) Formerly Graduate Student, Graduate School of Engineering, Hokkaido University. Now at Nippon Steel Corp. 3) Muroran R&D Lab., Nippon Steel Corp., 12 Nakamachi, Muroran, 050-8850 Japan.

(*Received on May 27, 2011; accepted on July 25, 2011*)

Effects of Nb addition on as-cast γ-austenite grain structure in 0.2 mass% carbon steel are investigated by means of furnace cooling and permanent mold casting experiments. In the furnace-cooled samples with Nb addition, Nb(C,N) particles crystallize from the last-solidifying liquid in non-equilibrium solidification condition and they act as pinning particles for γ grain growth just after the solidification completion. The Nb addition produces a strong pinning effect on the as-cast γ grain structure. In the permanent mold casting experiment, Coarse Columnar Grains (CCG) structure develops from the mold wall in the sample without Nb. The increase in Nb concentration gradually decreases the fraction of CCG region and increases the fraction of Fine Columnar Grains (FCG), thus leading to the grain refinement. This refinement could be ascribed to the pinning effect of Nb(C,N) particles.

KEY WORDS: solidification; casting; peritectic steel; pinning; grain refinement; austenite grain structure; columnar grain.

1. Introduction

As-cast γ-austenite structure in continuously cast slabs of peritectic carbon steels consists of Coarse Columnar Grains (CCG). Since the CCG structure causes the occurrence of surface cracking,[1,2)] the prevention of CCG formation is one of the most important issues in the field of solidification and casting of steels.

During the solidification of peritectic carbon steels, the liquid or δ-ferrite phase plays a role of a "pin" for γ grain growth in the liquid + γ or δ + γ two phase field. The substantial γ grain growth arises immediately after the liquid or δ phase vanishes below the temperature, T_γ, at which the peritectic transformation completes.[3–5)] In our recent study,[6)] the formation process of CCG structure during permanent mold casting of hyperperitectic carbon steels was investigated by means of a rapid unidirectional solidification method which realizes a cooling condition quite similar to that near the slab surface of practical continuously cast slabs. It was elucidated that the CCG structure forms by the mechanism of discontinuous grain growth. The solidifying microstructure is schematically illustrated in **Fig. 1**. The CCG structure develops below T_γ along the temperature gradient. In the temperature region between the peritectic reaction temperature T_p and T_γ, Fine Columnar γ Grains (FCG) exist ahead of the CCG. The liquid phase in FCG region prevents the FCG from growing along its short-axis direction. Hence, the short axis diameter of FCG is nearly equal to the primary Dendrite Arm Spacing (DAS) of δ dendrite. The liquid phase furthermore suppresses the vertical migration of FCG/CCG region boundary at which the temperature corresponds to T_γ. As the cooling proceeds, the position of T_γ moves away from the mold side and the FCG/CCG region boundary accordingly moves in the upward direction. The CCG thereby grow in the upward direction accompanied by the shrink of FCG near the FCG/CCG region boundary. There-

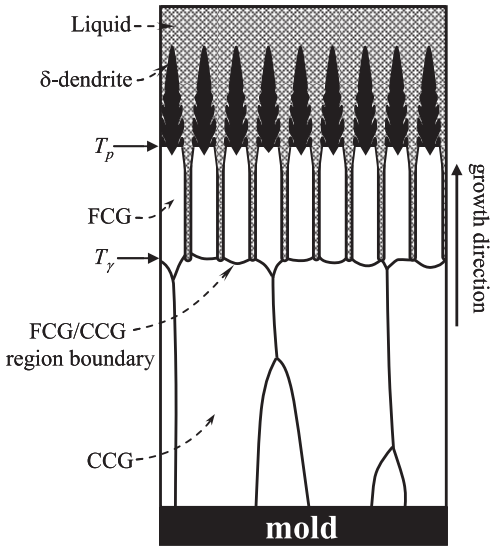

Fig. 1. Schematic illustration of growth process of CCG structure. T_p is the peritectic reaction temperature and T_γ is the temperature at which the peritectic transformation completes.

fore, the γ grain size at a fixed position suddenly increases by one order of magnitude from FCG to CCG when the local temperature falls below T_γ. This process can be classified as the discontinuous grain growth process under the temperature gradient.

As mentioned above, the CCG structure develops with the vertical motion of FCG/CCG region boundary shown in Fig. 1. Hence, the prevention of formation of CCG structure requires the motion of FCG/CCG region boundary to be retarded. This can be realized, for instance, by stabilizing liquid or δ phase in low temperature region, because the stabilized phase can act as a pin for γ grain growth as already mentioned above. In fact, our recent investigation by means of permanent mold casting of 0.2 mass% carbon steel demonstrated that the addition of Al and/or P stabilizes the liquid or δ phase in low temperature region and such a stabilized phase hinders the migration of the FCG/CCG region boundary, thus yielding the fine γ grain structure consisting of FCG over the whole cast.[7,8)]

In addition to the liquid or δ phase stabilized at low temperatures, carbonitride particles are expected to be useful in preventing the migration of FCG/CCG region boundary. In this paper, we focus on effects of Nb addition on the as-cast γ grain structure in 0.2 mass% carbon steel which is prone to exhibit coarse γ grain structure because of its high T_γ. Although the effects of Nb addition on as-cast γ grain size have been investigated in early studies,[9,10)] its effect on the motion of FCG/CCG region boundary has not attracted attention yet. Nb is well known as one of microalloying elements such as Ti and V which produce carbides, nitrides or carbonitrides and thus yield the pinning effect on low temperature structures.[10–14)] As shown later, the thermodynamic calculation indicates that Nb(C,N) is stabilized at relatively high temperatures by increasing Nb concentration in this steel. Hence, it is expected that Nb addition should give rise to the pinning effect on the γ grain growth during casting.

In this study, we carried out two types of cooling experiments, the slow and fast cooling experiments. In the former experiments, we attempt to reveal the formation process of Nb(C,N) during the solidification and cooling and its effect on the γ grain growth. In the latter experiment, we examine the effect of Nb addition on CCG formation process. One will see that Nb addition yields a substantial pinning effect on γ grain growth just after the liquid phase vanishes. Therefore, Nb addition is quite effective in preventing the migration of FCG/CCG region boundary and in refining the as-cast γ grain structure.

2. Experimental Procedures

The carbon steel used in this study is a hyperperitectic carbon steel of which the chemical composition is Fe–0.2%C–0.2%Si–0.8%Mn–0.015%P–0.04%Al–0.006%N (in mass%). The Nb concentration was varied from 0.0 to 0.5 mass%. P of 0.005 mass% was added to all the samples to make their P compositions to be 0.02 mass% P with an aim to observe the dendrite structure clearly. The effects of Nb addition on the as-cast γ grain structure were investigated by means of different cooling experiments, furnace cooling (slow cooling) and permanent mold casting (fast cooling) experiments as detailed below.

In the furnace cooling experiment, the sample of 130 g was put in an Al_2O_3 crucible with an inner diameter of 35 mm and a depth of 45 mm and it was melted at 1 550°C in a SiC electric furnace filled with Ar gas of five-nine purity. The sample was held for 1 h at 1 550°C, followed by cooling at a rate of 0.03°C/s. The samples were quenched from several temperatures ranging from 1 100 to 1 470°C into a strongly stirred iced water bath to investigate the γ grain growth during the cooling process. The quenched sample having a cylindrical shape was longitudinally sectioned and polished. After etching in a 3%-nitial solution, the microstructural observations were performed by means of an optical microscope. The average γ grain size, d_γ, was evaluated by the equivalent area diameter method and secondary Dendrite Arm Spacing (DAS), λ_2, was measured by the linear intercept method. Fine particles were identified and analyzed by a Scanning Electron Microscope (SEM) and an Electron Probe Micro Analyzer (EPMA).

In the permanent mold casting experiment, the sample of 250 g was put in a MgO crucible of cylindrical shape with an inner diameter of 30 mm and a depth of 90 mm. The sample was melted at 1 550°C in the SiC electric furnace under the Ar atmosphere. After holding for 1 h, the melt was cast into a steel mold held at room temperature. The mold has a cavity of rectangular prism shape and the details of mold shape and size can be found in Ref. 15). In the preliminary experiment, the cooling rates during this mold casting were estimated to be 5–30°C/s depending on the position of the sample. In order to observe the as-cast γ grain structure clearly, the martensite structure was obtained by quenching the sample into the strongly stirred iced water bath, when the temperature at the center of the ingot reaches about 1 100°C, for which the predetermined quenching timing was estimated from the preliminary temperature measurements.

The shape of the cast sample was the rectangular prism with a height of 40 mm, a width of 40 mm and a thickness of 20 mm. The quenched samples were sectioned horizontally at the middle of height. A rectangular area on the sectioned surface, extended from the mold side to the center in the thickness direction, was selected for the microstructural examination by the optical microscope, SEM and EPMA.

3. Results and Discussion

3.1. Furnace Cooling Experiment

The as-cast γ grain structures in the furnace-cooled samples without Nb and with 0.1 mass% Nb are shown in **Figs. 2**(a) and 2(b), respectively. These samples were quenched from 1 100°C. In each sample, the as-cast γ grains have

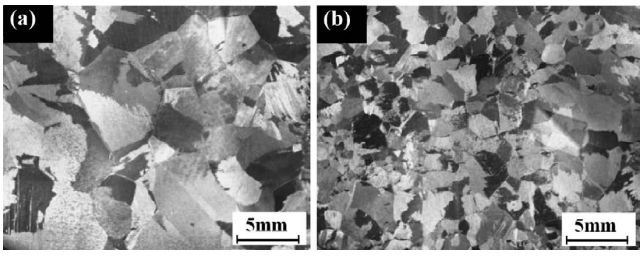

Fig. 2. γ grain structures in the samples (a) without Nb and (b) with 0.1 mass% Nb quenched from 1 100°C.

equiaxed shape. It is seen that the addition of Nb results in the reduction of γ grain size. **Figure 3** demonstrates the dependence of the γ grain size on the Nb concentration in the furnace-cooled samples quenched from 1 100°C. The filled square symbol indicates the result of Nb addition. The γ grain size gradually decreases with increase in Nb concentration. The addition of 0.1 mass% Nb decreases the γ grain size down to about one-half of the size without Nb addition. The dashed line represents the value of λ_2 which is almost independent of Nb concentration. The γ grain size seems to approach λ_2 as Nb concentration increases.

It should be pointed out that the refinement behavior shown in Fig. 3 is quite similar to that observed for the case of Ti addition.[16] In Fig. 3, the open circle symbols indicate the result of Ti addition reported in our recent paper.[16] The chemical composition of the steel, the experimental procedures and the cooling condition were the same as those in the present work. One can see that the grain refinement effect produced by Nb addition is as strong as that by Ti addition when the addition of 0.1 mass% is concerned. In the previous study on Ti addition, we found that in Ti-added samples, Ti(C,N) crystallizes from the liquid phase in high temperature region and it also appears from the last-solidifying liquid in low temperature region. The former phase is N-rich and has faceted shape, while the latter phase is C-rich and filmy shape. The thermodynamic calculations showed that the former phase crystallizes in liquid + δ + Ti(C,N) phase field, while the latter phase forms in liquid + γ + Ti(C,N) phase field. Importantly, the filmy-shaped Ti(C,N) always exists at the γ grain boundary during the cooling process and the grain refinement by Ti addition is entirely ascribable to the pinning effect of the filmy-shaped Ti(C,N).

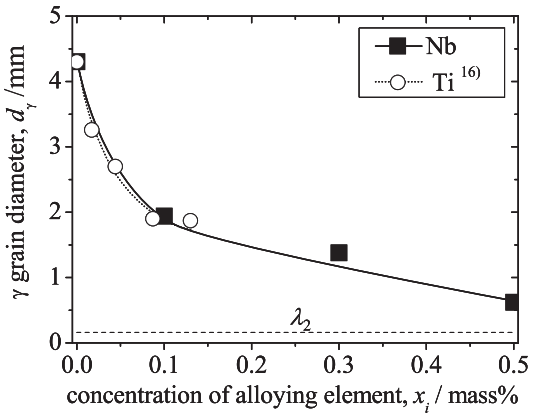

Fig. 3. Dependence of γ grain diameter on concentration of alloying element in the samples quenched from 1 100°C. The horizontal dashed line represents the value of secondary DAS, λ_2, which is almost independent of the concentration.

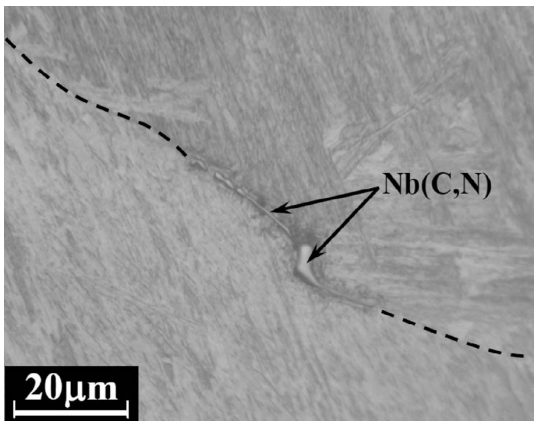

Fig. 4. Nb(C,N) phase observed in the sample with 0.1 mass% Nb quenched from 1 100°C. The γ grain boundary is specified by the dashed line for visual aid.

Figure 4 shows the micrograph of the particles observed in the sample with 0.1 mass% Nb quenched from 1 100°C. The dashed lines indicate the γ grain boundary. The particles have filmy shape and they are located at the γ grain boundary. The result of EPMA analysis of these particles is shown in **Table 1**. It was identified as Nb(C,N) phase. The Nb(C,N) particles of filmy shape were observed in all the samples with Nb addition and they always exist at the γ grain boundary. As is similar to the case of Ti addition, hence, it is considered that the refinement of as-cast γ grain structure shown in Fig. 3 should be ascribed to the pinning effect of these filmy-shaped Nb(C,N) particles.

The phase diagram for Fe–0.2%C–0.2%Si–0.8%Mn–0.04%Al–0.006%N–*x*Nb calculated by the CALPHAD method[17] is shown in **Fig. 5**. The thermodynamic database, PanIron,[18] was used for this calculation. Nb(C,N) phase is stabilized at high temperatures by addition of Nb. It crystallizes from the liquid phase at Nb concentrations higher than about 0.32 mass%. According to the phase diagram, when Nb concentration is 0.1 mass%, Nb(C,N) phase precipitates from γ phase below 1 300°C. Therefore, in the equilibrium solidification condition, the pinning effect of Nb(C,N) phase, if any, should arise in low temperature region after the substantial grain growth occurs. As shown in Fig. 3, however, the grain refinement was observed even in the sample with 0.1 mass% Nb. Also, the filmy-shaped Nb(C,N) particles were found in the sample with 0.1 mass% Nb (Fig. 4). Judging from their shape and size, it is considered that these Nb(C,N) particles crystallized from the liquid phase.

In order to clarify the formation process of Nb(C,N) and

Table 1. Result of composition analysis of particle.

	C	Nb	N	Si	Mn	Al	P
Composition /at%	35.7	57.7	1.1	0.02	0.07	5.4	1.1

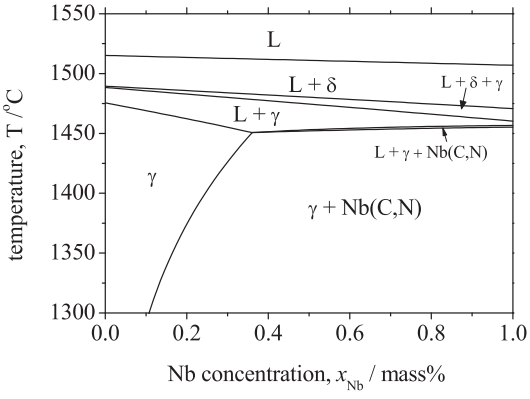

Fig. 5. Phase diagram of Fe–0.2C–0.2Si–0.8Mn–0.04Al–0.006N–*x*Nb calculated by the CALPHAD method.

its effect on the grain growth, we investigate γ grain structure at several temperatures during the cooling process. The results are demonstrated in **Fig. 6**. One can see that in the sample without Nb addition, the γ grain growth significantly occurs below 1 450°C at which the liquid phase almost vanishes. In the samples with 0.1 mass% Nb, however, the grain growth was retarded in high temperature region. More specifically, at 1 300°C, the grain size in the sample with 0.1 mass% Nb is obviously smaller than that without Nb. Also, the growth does not virtually take place below 1 300°C. The grains do not grow at all over the whole temperature range in the sample with 0.5 mass%. The half-filled circle symbols indicate the results of Ti addition,[16] which are quite similar to the results of 0.1 mass% Nb. As already mentioned, in Ti-added sample, the filmy-shaped Ti(C,N) particles crystallize from the last-solidifying liquid and they are always located at the γ grain boundary during the cooling, thus providing the strong pinning effect.[16] The similar behavior was actually observed in the present case. A trace of the residual liquid phase in the sample with 0.1 mass% Nb is shown in **Fig. 7**. The sample was quenched from 1 470°C. The dark region corresponds to the residual liquid phase which is located at the γ grain boundaries. Inside the residual liquid phase, also, Nb(C,N) crystals exist as indicated in the figure. Although these Nb(C,N) crystals might form during the quenching operation, the existence of Nb(C,N) in Fig. 7 is considered to indicate the possibility that Nb(C,N) crystallizes from the liquid below 1 470°C in this sample. In fact, it was observed that at the lower temperature of 1 450°C, the liquid phase almost vanishes and coarse Nb(C,N) particles of filmy shape appear at the γ grain boundary instead. Therefore, Nb(C,N) particles shown in Fig. 4 crystallized from the last-solidifying liquid, which may occur under non-equilibrium solidification condition involving segregation of Nb.

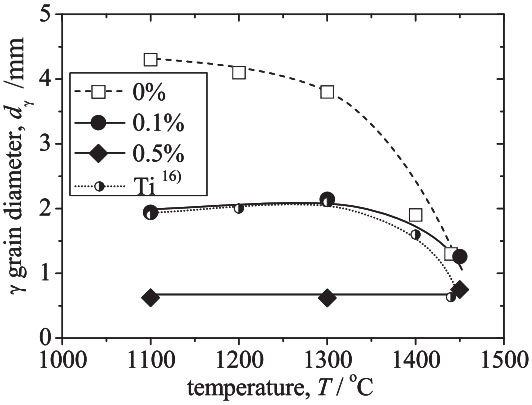

Fig. 6. Temperature dependence of γ grain diameter in the samples with different Nb concentrations. The data of 0.09 mass% Ti[16] is also plotted for the comparison.

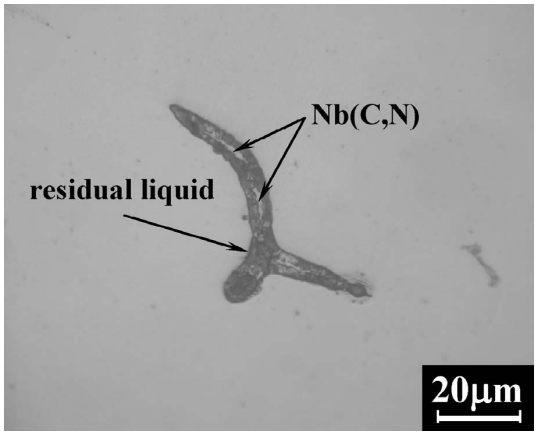

Fig. 7. Residual liquid phase (dark region) observed in the sample with 0.1 mass% Nb quenched from 1 470°C. Nb(C,N) crystal which might form during the quenching operation is seen inside the residual liquid.

As discussed in the previous report,[16] the γ grain size in the sample with Ti addition is dependent on the amount of filmy Ti(C,N) particles. This fact should be applied to the present case of Nb addition. The amount of Nb(C,N) crystallizing during cooling should increase with increase in amount of Nb addition. In fact, as shown in Fig. 6, the γ grains grow to be about 2 mm in size during the cooling in the sample with 0.1 mass% Nb, while the γ grain growth does not virtually occur in the sample with 0.5 mass% Nb.

The results are briefly summarized as follows. The γ grain size at 1 100°C is reduced by Nb addition (Fig. 3). The reduction is substantial even in the sample with 0.1 mass% Nb. In Nb-added samples at 1 100°C, Nb(C,N) particles of filmy shape exist at the γ grain boundary (Fig. 4). Such Nb(C,N) particles appears in high temperature region just after the liquid phase vanishes and γ grain growth is retarded even at high temperatures (Fig. 6). According to these facts, we can conclude that Nb(C,N) particles crystallize from the last-solidifying liquid under non-equilibrium solidification condition and they act as a pining phase for γ grain growth during cooling. This is quite similar to what we found for the case of Ti addition in which the pinning particle is Ti(C,N). The grain refinement effect by Nb addition is as strong as that by Ti addition as shown in Figs. 3 and 6.

As described above, non-equilibrium solidification takes place even at the slow cooling rate of 0.03°C/s which facilitates the crystallization of Nb(C,N). In the faster cooling process of the permanent mold casting, hence, it is highly expected that strong pinning effect of Nb(C,N) emerges in Nb-added sample and considerably affects the motion of FCG/CCG region boundary.

3.2. Permanent Mold Casting Experiment

The main concern of this study is utilization of pinning effect induced by Nb addition for suppression of the migration of FCG/CCG region boundary. The as-cast γ grain structures in the samples after the permanent mold casting are shown in **Fig. 8**. The bottom of each micrograph is the mold side, while the upper side corresponds to the center of the ingot. The solidification unidirectionally proceeds from the bottom to upper side which was confirmed by the fact that the columnar dendrites unidirectionally develops from the mold side to the center of ingot. In the sample without Nb addition (Fig. 8(a)), the CCG, of which the average short-axis diameter is about 1 mm, develop from the mold side in the upper direction and the Equiaxed Grains (EG) form in the center part of the ingot. The γ grain structure drastically changes by Nb addition. The addition of 0.1 mass% Nb results in the formation of Fine Columnar γ Grains (FCG) in between the CCG and EG regions. The further addition of Nb yields the reduction of CCG region. The

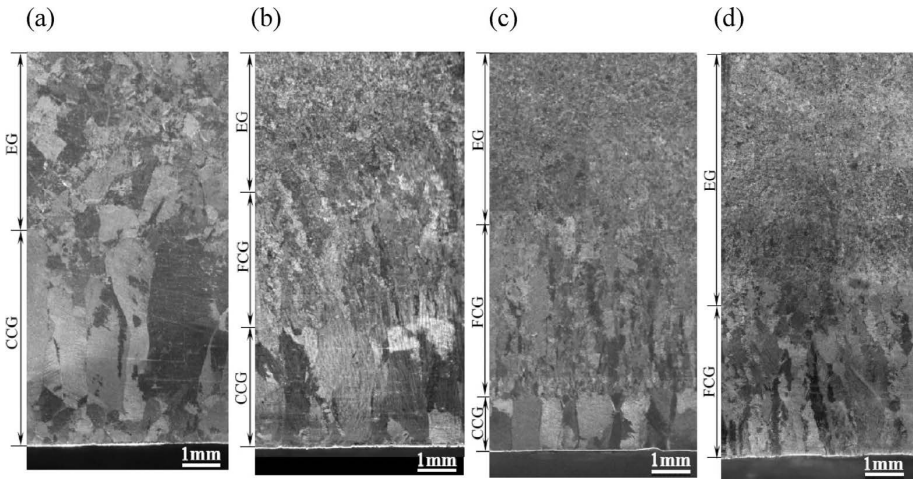

Fig. 8. As-cast γgrain structures in the samples with (a) 0 mass% Nb, (b) 0.1 mass% Nb, (c) 0.3 mass% Nb and (d) 0.5 mass% Nb. CCG, EG and FCG stands for coarse columnar grains, equiaxed grains and fine columnar grains.

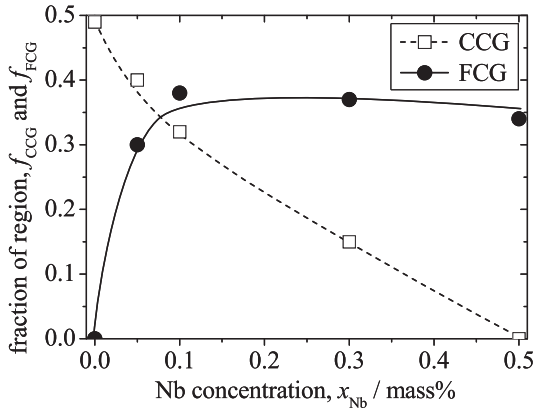

Fig. 9. Dependence of fractions of CCG and FCG regions on Nb concentration.

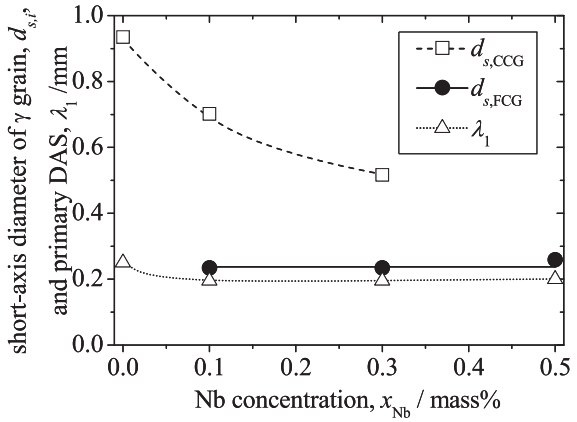

Fig. 10. Dependences of short-axis diameters of CCG, FCG and primary DAS on Nb concentration.

CCG region vanishes in the sample with 0.5 mass% Nb in which the structure consists of only the FCG and EG regions.

The length of each region along the thickness direction of ingot was measured and divided by the total length of the observation area, 10 mm, to estimate the fraction of region, f_i with i = CCG and FCG. The results are shown in **Fig. 9**. The fraction of CCG region gradually decreases with increase in Nb concentration. The CCG do not exist in the sample with 0.5 mass% Nb. The fraction of FCG region drastically increases up to 0.3 by addition of 0.05 mass% Nb and then it takes almost a constant value of about 0.35–0.4.

Figure 10 shows the dependences of short-axis diameters of CCG and FCG and the primary DAS on Nb concentration. The short-axis diameter of FCG and the primary DAS represent the values measured at about 4 mm away from the mold side. The short-axis diameter of CCG gradually decreases with increase in Nb concentration. Whereas, both the short-axis diameter of FCG and the primary DAS take almost constant values. Importantly, the short-axis diameter of FCG is almost equivalent to the primary DAS. The dendrite and γgrain structures in FCG region in the sample with 0.3 mass% Nb are shown in **Figs. 11**(a) and 11(b), respectively. Also, the schematic illustration of these structures is shown in Fig. 11(c). One can see the grain boundaries of

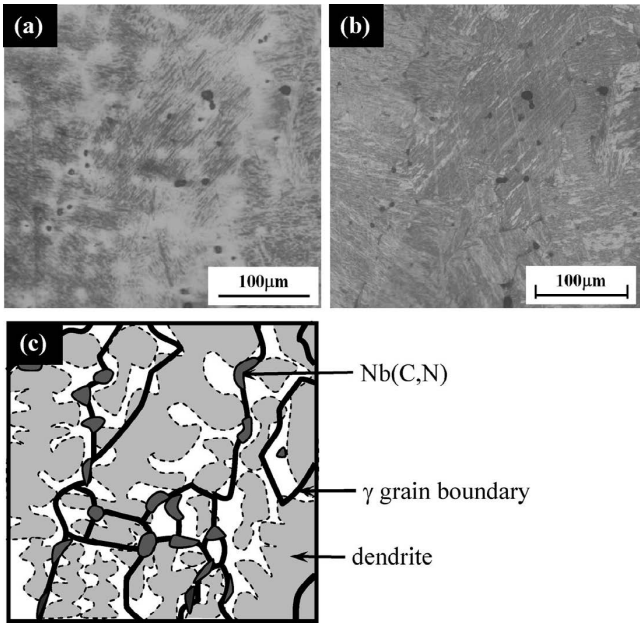

Fig. 11. (a) Dendrite, (b) γgrain structures at the same position of FCG region in the sample with 0.3 mass% Nb. (c) Schematic illustration of both the structures in which Nb(C,N) particles are drawn larger than the reality to make them visible.

FCG are mostly located at the interdendritic positions. Furthermore, most Nb(C,N) particles are located at the interdendritic positions and the γ grain boundaries. As discussed in section 3.1, Nb(C,N) crystallizes from the last-solidifying liquid and it works as a pinning particle for γ grain growth during the slow cooling process. Figure 11 demonstrated that this fact can be applied to the case of the permanent mold casting process. The Nb(C,N) particle crystallizes at the interdendritic region and it prevents the FCG from growing along its short-axis direction, making the short-axis diameter of FCG comparable to the primary DAS. Therefore, the formation of FCG structure due to Nb addition shown in Fig. 8 should be attributed to the pinning effect of Nb(C,N) crystallizing at the interdendritic region.

The existence of Nb(C,N) particle should be effective not only in preventing the growth of FCG along its short-axis direction but also in inhibiting the migration of FCG/CCG region boundary. **Figure 12** is the SEM micrograph of the γ grain structure in the vicinity of FCG/CCG region boundary. The upper and lower parts correspond to the FCG and CCG regions, respectively. The bright particles were identified as Nb(C,N). A number of Nb(C,N) particles are dispersed in the vicinity of FCG/CCG region boundary. It is considered that these particles pinned the migration of FCG/CCG region boundary. In particular, the appearance of FCG structure in as-cast samples shown in Fig. 8 implies that the migration of FCG/CCG region boundary was completely suppressed during the cooling process. The pinning effect of Nb(C,N) particles on FCG/CCG region boundary is analyzed below.

The migration velocity of FCG/CCG region boundary, V_γ, during the CCG formation process illustrated in Fig. 1 is first discussed. The migration velocity of the grain boundary is proportional to the curvature of the boundary often described by the reciprocal of the grain radius.[19] As is commonly (sometimes implicitly) done in the theories of grain growth,[19,20] we assume that the triple junction lines and quadruple junction points of γ grain boundaries do not affect the kinetics of the grain growth. Then, V_γ is entirely controlled by the shrinking velocity of FCG adjoining CCG region. Consequently, V_γ is written as[21]

$$V_\gamma = m\left(T^*\right)\frac{\sigma}{\xi \cdot d_{s,FCG}} \quad \text{..... (1)}$$

where $m(T^*)$ is the grain boundary mobility at a temperature T^* and σ is the grain boundary energy, $d_{s,FCG}$ is the short-axis diameter of FCG. Here T^* refers to the temperature at the FCG/CCG region boundary. ξ is a constant depending on the shape of FCG/CCG region boundary. From the analysis on the shape of FCG/CCG region boundary, ξ can be approximated to be $\xi = 0.78$. The validity of Eq. (1) is fully supported by the phase-field simulations for the discontinuous grain growth.[21] The detail about the derivation of Eq. (1) will be described elsewhere.[21] Here, it is noticed that $d_{s,FCG}$ in Eq. (1) is nearly equal to λ_1 as shown in Fig. 10. Hence, the velocity of FCG/CCG region boundary is inversely proportional to λ_1 according to Eq. (1). λ_1 essentially depends on the cooling condition and thus the position of the ingot. **Figure 13** demonstrates the dependence of λ_1 on the distance from the mold wall, l, in the sample without Nb addition. This spatial profile of λ_1 does not significantly change with Nb concentration as is exemplified in Fig. 10. λ_1 gradually increases with the distance from the mold wall. Therefore, the velocity of FCG/CCG region boundary given by Eq. (1) gradually decreases with the distance from the mold wall. In other words, the driving force of CCG formation decreases with the distance from the mold wall. In fact, the EG region develops in the center region of the sample without Nb addition as shown in Fig. 8(a), which can be explained by the low driving force of CCG formation in the center region.

Now, we estimate the pinning pressure required for the complete suppression of migration of FCG/CCG region boundary. When the pinning effect exists, V_γ is reduced according to the following equation,

$$V_\gamma = m\left(T^*\right)\left(\frac{\sigma}{\xi \cdot \lambda_1} - P_{pin}\right), \quad \text{..... (2)}$$

where P_{pin} represents the pinning pressure exerted on the FCG/CCG region boundary. $d_{S,FCG}$ in Eq. (1) is replaced by λ_1 in Eq. (2). Therefore, in order for the migration of FCG/CCG region boundary to be completely suppressed, the following relation should be satisfied,

$$P_{pin} = \frac{\sigma}{\xi \cdot \lambda_1} \quad \text{..... (3)}$$

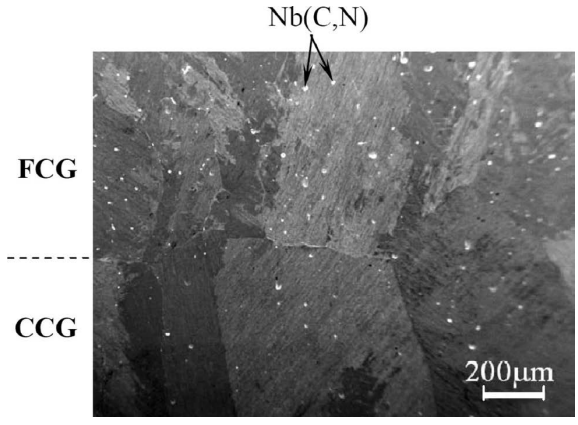

Fig. 12. SEM micrograph in the vicinity of FCG/CCG region boundary.

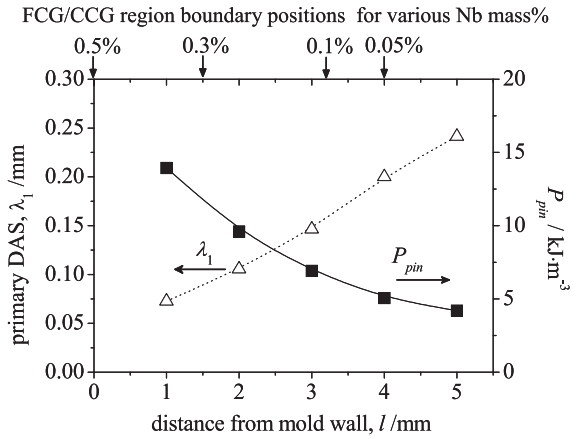

Fig. 13. Primary DAS and the corresponding pinning pressure required for complete suppression of FCG/CCG region boundary migration versus distance from mold wall. The positions of FCG/CCG region boundary observed in the samples with different Nb concentrations are indicated in the upper part of the figure.

This is the pinning pressure required for the complete suppression of the migration of FCG/CCG region boundary, which is inversely proportional to λ_1. Using the measured value of λ_1 shown in Fig. 13, then, P_{pin} can be calculated from Eq. (3). The result of P_{pin} is shown in Fig. 13. In this calculation, σ was set to be $\sigma = 0.79$ J·m^{-2}.[22] One can see that the pinning pressure required for the complete suppression of the migration of FCG/CCG region boundary gradually decreases with the distance from the mold wall. In the casting experiment, hence, if Nb(C,N) produces the strong pinning effect, the migration of FCG/CCG region boundary can be stopped in the vicinity of the mold wall. However, if the pinning pressure of Nb(C,N) is low, the FCG/CCG region boundary should continue to migrate or be stopped near the center of the ingot. The pinning pressure essentially depends on the amount of the pinning particles and their size. It is generally expected that the addition of larger amount of Nb yields higher volume fraction of Nb(C,N) particle and thereby higher pinning pressure on FCG/CCG region boundary. In the upper part of Fig. 13, the positions of the FCG/CCG region boundary observed in the samples with different Nb concentrations are indicated. It is seen that the observed position of completely suppressed FCG/CCG region boundary approaches the mold side as the Nb concentration increases. Hence, this result suggests that the gradual reduction of CCG region by Nb addition shown in Fig. 9 can be explained by the increment of pinning pressure due to Nb addition, although the discussion is qualitative.

4. Conclusions

It was found in the recent study that the coarse columnar γ grains (CCG) structure originates from the discontinuous grain growth which is characterized by the motion of the boundary between the CCG and the fine columnar γ grains (FCG) regions.[6] Therefore, the prevention of the development of CCG structure requires the migration of FCG/CCG region boundary to be inhibited, which should be realized by the pinning effect of carbonitride. In the present study, we have investigated the effects of Nb addition on the as-cast γ grain structure in the 0.2 mass% carbon steel. The following are the important findings in this study.

(1) In the samples with Nb concentration from 0.1 to 0.5 mass%, the solidification proceeds in non-equilibrium condition even at the slow cooling rate of 0.03°C/s, which facilitates the crystallization of Nb(C,N) from the last-solidifying liquid. The Nb(C,N) phase takes the filmy shape during the slow cooling process.

(2) The pinning effect of Nb(C,N) particle emerges just after the liquid phase vanishes. Hence, the Nb addition produces the grain refinement effect on as-cast γ grain structure even at high temperatures.

(3) The CCG structure forms during the permanent mold casting. The Nb addition reduces the fraction of CCG region and it increases the fraction of FCG region.

(4) The growth of FCG along its short-axis direction is inhibited by Nb(C,N) crystallizing at the interdendritic region.

(5) Nb(C,N) phase may inhibits the migration of FCG/CCG region boundary, thus reducing the fraction of CCG region.

Acknowledgement

This work is supported by Grant-in-Aid for Young Scientists (A) (No. 22686067) from MEXT, Japan.

REFERENCES

1) B. Mintz and J. M. Arrowsmith: *Met. Technol.*, **6** (1979), 24.
2) L. Schmidt and Å. Josefsson: *Scand. J. Metall.*, **3** (1974), 193.
3) Y. Maehara, K. Yasumoto, Y. Sugitani and K. Gunji: *Trans. Iron Steel Inst. Jpn.*, **25** (1985), 1045.
4) K. Yasumoto, T. Nagamichi, Y. Maehara and K. Gunji: *Tetsu-to-Hagané*, **73** (1987), 1738.
5) N. S. Pottore, C. I. Garcia and A. J. DeArdo: *Metall. Trans.*, **22A** (1991), 1871.
6) S. Tuchiya, M. Ohno, K. Matsuura and K. Isobe: *Acta Mater.*, **59** (2011), 3334.
7) S. Kencana, M. Ohno, K. Matsuura and K. Isobe: *ISIJ Int.*, **50** (2010), 231.
8) S. Kencana, M. Ohno, K. Matsuura and K. Isobe: *ISIJ Int.*, **50** (2010), 1965.
9) K. Narita, A. Miyamoto, F. Kawaguchi and S. Nasu: *Tetsu-to-Hagané*, **47** (1961), 1512.
10) K. Narita and A. Miyamoto: *Tetsu-to-Hagané*, **50** (1964), 174.
11) Y. Ogino, H. Tanida, M. Kitaura and A. Adachi: *Tetsu-to-Hagané*, **57** (1971), 533.
12) H. Kaji, S. Kinoshita and N. Hayashi: *Tetsu-to-Hagané*, **58** (1972), 1759.
13) H. Kobayashi and Y. Kasamatu: *Tetsu-to-Hagané*, **67** (1981), 1990.
14) K. Banerjee, M. Militzer, M. Perez and X. Wang: *Metall. Mater. Trans. A*, **41A** (2010), 3161.
15) M. Ohno and K. Matsuura: *ISIJ Int.*, **48** (2008), 1373.
16) S. Tsuchiya, M. Ohno, K. Matsuura and K. Isobe: *Tetsu-to-Hagané*, **95** (2009), 629.
17) L. Kaufman and H. Bernstein: Computer Calculation of Phase Diagrams with Special Reference to Refractory Materials, Academic Press, New York, (1970), 1.
18) http://www.computherm.com/databases.html
19) M. Hillert: *Acta Metall.*, **13** (1965), 227.
20) J. W. Cahn: *Acta Metall. Mater.*, **39** (1991), 2189.
21) M. Ohno, S. Tsuchiya and K. Matsuura: *Acta Mater.*, **59** (2011), 5700.
22) E. D. Hondros: *Proc. R. Soc. (London) A*, **A286** (1965), 479.